Zeolites

Deutsche Ausgabe: DOI: 10.1002/ange.201707452
Internationale Ausgabe: DOI: 10.1002/anie.201707452

CIT-9: A Fault-Free Gmelinite Zeolite

Michiel Dusselier, Jong Hun Kang, Dan Xie, and Mark E. Davis**

Abstract: *A synthetic, fault-free gmelinite (GME) zeolite is prepared using a specific organic structure-directing agent (OSDA), cis-3,5-dimethylpiperidinium. The cis-isomers align in the main 12-membered ring (MR) channel of GME. Trans-isomer OSDA leads to the small-pore zeolite SSZ-39 with the OSDA in its cages. Data from N_2-physisorption and rotation electron diffraction provide evidence for the openness of the 12 MR channel in the GME 12×8×8 pore architecture and the absence of stacking faults, respectively. CIT-9 is hydrothermally stable when K^+-exchanged, while in the absence of exchange, the material transforms into an aluminous AFI-zeolite. The process of this phase-change was followed by in situ variable temperature powder X-ray diffraction. CIT-9 has the highest Si/Al ratio reported for GME, and along with its good porosity, opens the possibility of using GME in a variety of applications including catalysis.*

Zeolites and other microporous molecular sieves continue to find new uses in catalysis, sorption, and specialty applications.[1] Besides their dominant presence in petrochemistry,[2] their potential in the conversion of renewables[3] or gas is huge,[4] and often a single framework excels at a specific task. Although new structures are being reported frequently, for some long-known topologies, no effective synthesis has been reported yet. Natural occurring gmelinite, as well synthetic aluminosilicates with the GME topology, nearly always display stacking faults (CHA intergrowths) blocking the main channel and thus limiting porosity. The search for fault-free, synthetic GME has been going on for 40 years because the framework is a three-dimensional 12×8×8 channel system with promise for relevant hydrocarbon chemistries, for example, hexane isomerization and molecular traffic control (compare to LTL).[1b] Using a cationic dabco-polymer as OSDA, Mobil presented a new route to synthetic GME in 1978.[5] Later, Chiyoda and Davis reported a hydrothermal interzeolite conversion route from zeolite Y (induced by Sr^{2+}), and benchmarked faulting via electron diffraction and sorption, against both dabco-GME and gmelinite.[6] All materials showed faulting to some extent, even dabco-GME, that showed a micropore volume (N_2-adsorption, NA^+-form) there of only 0.055 $cm^3 g^{-1}$.[6] We here present a convenient new method, based on a straightforward OSDA, that is, *cis*-3,5-dimethylpiperidinium hydroxide, that produces fault-free GME zeolites, denoted CIT-9, with high porosity of over 0.17 $cm^3 g^{-1}$. Moreover, a fair comparison with dabco-GME (0.12 $cm^3 g^{-1}$) made in our hands, and Sr-GME, confirms the absence of faulting in CIT-9 while some disorder is present in all other known GME zeolites.

Earlier, we reported the role of geometric *cis*/*trans*-isomerism of dimethylpiperidinium-derived OSDAs in the synthesis of zeolite SSZ-39, a useful small-pore zeolite (AEI) with large cages.[7] It was shown that *cis*-3,5-dimethylpiperidinium and different mixtures of *cis*/*trans*-3,5-dimethylpiperidinium, and even *cis*-2,6-dimethylpiperidinium could direct toward SSZ-39.[7,8] In this work, by increasing the OSDA concentration in very similar syntheses and using only the pure *cis*-3,5 isomer, GME zeolites were prepared (Figure 1 A, upper trace). Remarkably, the competition between AEI and GME was influenced by the concentration of the synthesis mixture. While keeping all parameters constant but adding less water, that is, going from bottom (AEI) to top in Figure 1 A, GME turns out to be the dominant zeolite grown. The difference in getting pure GME or pure AEI is the molar H_2O/Si ratio going from 20 to 35. Although it is hard to pinpoint this dilution effect on a specific compound in the synthesis mixture, cross-parameter experiments (Table S1 in the Supporting Information) showed that the concentration of OSDA is the most prominent factor determining the type of zeolite, as a phase-selectivity versus concentration plot indicates (Figure 1 B). The sigmoidal plot confirms the unusually sensitive phase-selectivity in a case where both

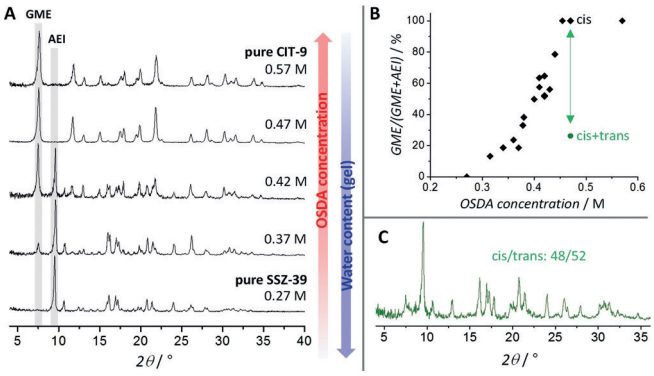

Figure 1. A) Powder X-ray diffraction (PXRD) of final product with *cis*-3,5 OSDA and varying water content. B) Relative GME selectivity with respect to AEI from major reflections in A and Figure S3 in function of OSDA concentration. C) 0.47 M synthesis with 48/52 mixture of *cis*/*trans*-3,5-OSDA (green dot in B).

[*] Dr. M. Dusselier, J. H. Kang, Dr. M. E. Davis
Chemical Engineering, California Institute of Technology
1200 E. California Blvd., Pasadena, CA 91125 (USA)
E-mail: mdavis@cheme.caltech.edu
Dr. M. Dusselier
Center for Surface Chemistry and Catalysis, KU Leuven
Celestijnenlaan 200F, Heverlee, 3010 (Belgium)
E-mail: michiel.dusselier@kuleuven.be
Dr. D. Xie
Chevron Energy Technology Company
100 Chevron Way, Richmond, CA 94802 (USA)
Supporting information and the ORCID identification number(s) for the author(s) of this article can be found under https://doi.org/10.1002/anie.201707452.

products are structure-directed by the same OSDA and also retain this organic in the structure [either in pores (GME) or cages (AEI)]. A detailed synthetic account is found in the Supporting Information (Sections 3.1–3.4, Table S2, and Figures S1–S4).

Besides remarkable concentration dependence within the *cis*-isomer series, the synthesis of CIT-9 is very geometric isomer-sensitive as the presence of *trans*-3,5-OSDA leads to SSZ-39 even at higher OSDA concentration (Figure 1 C). The latter is in line with recent AEI studies, where OSDA mixtures high in *trans* were crystallizing significantly faster than *cis* ones.[7,8b] Here, the large effect, that is, an entirely different type of zeolite rather than a different rate, for only a small molecular change in the OSDA is remarkable. Molecular modelling calculations firmly support these experiments, and offer an explanation for the results obtained. Distinctly lower energies and a more snug fit of 2 *cis*-OSDAs, opposed to *trans*, are found in the unit cell of GME (Figure 2).

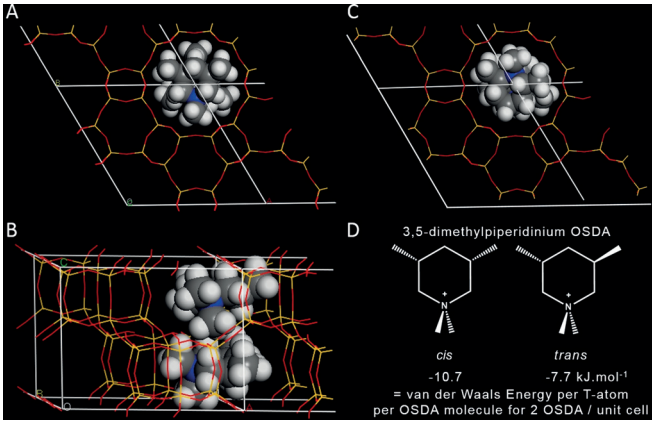

Figure 2. A,B) Commensurate fit of two *cis*-3,5-OSDA molecules in the 12MR channel of GME. C) *trans*-3,5 isomer fit. D) OSDAs and resulting energies.

The excellent fit of the *cis*-molecules, visually evident looking down in the 12MR channel of GME (Figures 2 A, S5), results in a large 3 kJ mol^{-1} difference in stabilization energy with the *trans*-isomer (Figures 2 C,D). Usually, 2 kJ mol^{-1} differences between chemically-different OSDA and a specific framework are considered sufficient to support experimentally diverging syntheses.[9] Here, the larger difference, caused only by *cis*/*trans* isomerism is unprecedented in the zeolite literature.[10] The molecular modeling provides a further clue into the selectivity of the *cis*-OSDA for both GME and AEI, respectively in concentrated and dilute conditions. The energies are most favorable for GME using two organics per unit cell, instead of less, implying OSDAs closely line up in the large pore (Figure 2 B). It is likely that this type of structure-direction is only possible when the concentration in the synthesis liquid is high. Dilute conditions lead to AEI, where each cage contains one organic.[7,11] Remarkably, the framework densities of both topologies are identical (15.1 T-atoms/1000 Å^3), and both can be entirely constructed from only the double 6-ring (*d6r*) composite building unit (as are CHA, AFX, … and remarkably FAU, the Al-source here). Likely, these similarities allow for the synthesis to easily lead to either GME or AEI, and increase sensitivity to the OSDA, both its isomer form and concentration. Solid state ^{13}C-NMR spectra of the *cis*-OSDA inside CIT-9 (Figure S6) reveal that the OSDA remains intact and about 1.5 OSDAs per unit cell were measured from thermogravimetric analysis (TGA; Figure S7).

A faulted or disordered nature, reported to some extent for all existing GME-zeolites,[6] lowers micropore volume and thus the accessibility of the material. This property has hampered the exploitation of GME for study in catalysis and other applications. A full characterization of CIT-9, with emphasis on disorder, revealed its superiority with respect to the known GME-zeolites. We synthesized dabco-GME[5] for comparison since it was speculated to have low faulting because of its adsorption properties (no structural analyses were reported). Here, we assess the extent of disorder by rotation electron diffraction (RED; other dabco-GME data, see Figures S8 and S9).The RED data for CIT-9 (Figure 3 A) show no evidence of disorder or faulting. No streaking is observed along the three axes, and this is especially important in the c-dimension to ensure an open 12MR channel (enlarged, Figure S10). Dabco-GME shows some signs of faulting, mainly along the c-axis, while a lot of disorder is evident in Sr-GME (Figures 3 B,C). Both the latter and gmelinite are known to be heavily faulted and this is even visible in classic PXRD (Figure S11).

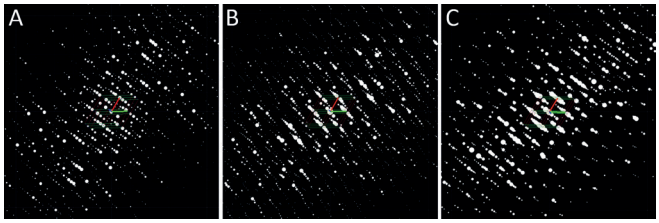

Figure 3. RED showing A) no disorder in CIT-9; B) some disorder in dabco-GME along c; and C) a lot of disorder along c in Sr-GME. Unit cell with a, b-axis in red and green, respectively, looking down in c.

To assess porosity, both dabco-GME and CIT-9 were subjected to a range of thermal treatments prior to N_2-physisorption. It became apparent that after calcination (580 °C) to remove OSDA, both GME materials had transformed into another phase, the AFI zeolite, with similar diffraction distances. Literature documents this for both dabco-GME[12] and gmelinite.[13] Alberti et al. for example, studied dehydration of the mineral and noted AFI formation above 300 °C.[13] In case of synthetic materials, OSDA molecules are still present in the pores during heating before they combust. To this point, the mechanism of the GME to AFI transformation has not been studied. A custom cell allowed PXRD to be tracked under heating (Figure 4 A, S12) to study the thermal behavior of CIT-9. The dataset consistently shows that reflections relating to the a and b-axes of the GME unit cell shift to the left, indicating expansion along a and b (e.g. *210* and *110*) while the c-axis shrinks (right shift of *002*), from 30 °C to 230 °C. Pure AFI is found from

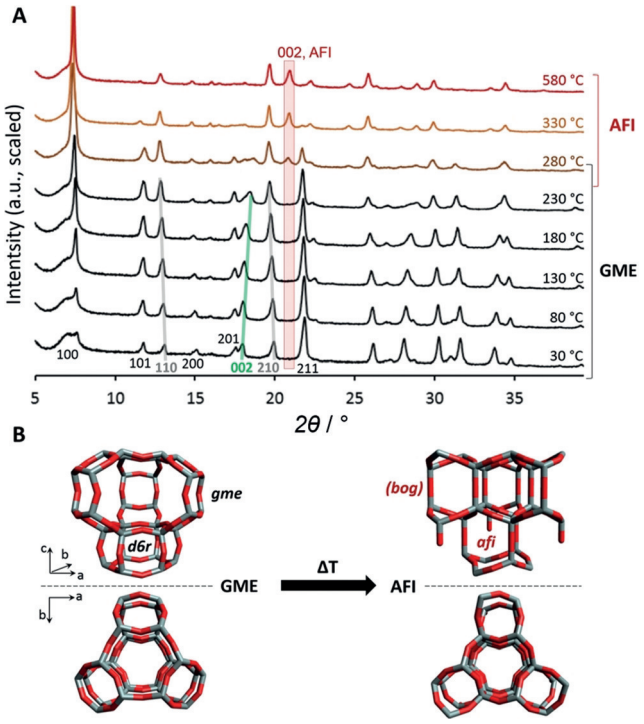

Figure 4. A) Variable-temperature XRD of CIT-9 with key reflections of GME shifting right or left, before transformation to AFI (Figure S12). B) Structural details of the transformation seen from the joined *d6r* + *gme* units in GME. Top view (see fit with 12MR channel in Figure 2A) shows similarity between GME and AFI.

330 °C onward, with no further change between 330 and 580 °C or after cooling. The mechanism thus invokes compressing the *gme* cage, and breaking and reforming at least 18 T–O bonds in the *gme-d6r* stack to reshuffle it into an *afi* (and part *bog*) cavity (Figure 4B). Likely, the aluminous and polar nature of the framework allows this to occur. Interestingly, aluminosilicate AFI is not accessible from synthesis in the low Si/Al region, and is usually found as pure silicate[14] or with boron. Often, postsynthetic alumination needs to be performed before catalysis.[15] Here, steaming and dealumination could lead to a range of new Si/Al ratios (4–50) for AFI zeolites for example, for gas adsorption applications.

Although scientifically fascinating, the transformation during calcination implies that the GME framework cannot be emptied for catalysis and sorption applications. To circumvent this, two approaches were successful. First, an ozone-treatment (flowing) at 150 °C allowed nearly full removal of OSDA without the transformation to AFI occurring. Afterward, the GME materials (CIT-9 and dabco-GME) were assessed with N_2-physisorption. Multiple repeats, samples and setups (Table S3) showed an average micropore volume of 0.17 $cm^3 g^{-1}$ for CIT-9 versus only 0.12 $cm^3 g^{-1}$ for dabco-GME. The 40 % higher volume of CIT-9 is consistent with the higher faulting in dabco-GME as measured by RED, and the more open nature of the CIT-9 versus the more disordered dabco-GME. The ozone-treated materials could easily be ion-exchanged using classic protocols, rendering GME available in all forms for use below 280 °C. In the K^+-form however, GME proved to be thermally stable (e.g., at 580 °C). The stabilizing effect of K^+ is not surprising as K^+ fits into *gme*-cavities and/or its 8MR windows, and once there, could prevent the compression and bond-reforming needed for AFI formation (Figure 4B, AFI has no 8MR). K^+-exchanged, but non-calcined samples showed a decreased pore volume, hinting to obstruction of the main 12MR channel. Calcination likely drives K^+ into the side-cages and out of the 12MR pore system, as 0.15 $cm^3 g^{-1}$ was obtained for calcined K^+-CIT-9 (Figure S13). Similar findings have been shown for LTL zeolites.[16] The second approach to an open-GME was based on a method by Huo et al.[17] This relies on slowly calcining a slurry of the organic-filled GME with a hyper-concentrated KCl salt. This procedure works for CIT-9 and leads to a stable, porous K^+-GME in one step (0.15 $cm^3 g^{-1}$, Figures S14–S16).

CIT-9 can be made with Si/Al ratios up to 4.0 (EDX; see Sections 3.2 and 3.4 in the Supporting Information). In contrast, synthetic Sr- and dabco-GME, and gmelinite have a molar Si/Al in the range of 2.0–3.0 (Table S4).[5] This difference, up to about one aluminum less per unit cell, potentially improves its stability. ^{29}Si-NMR confirmed the Si/Al differences between GME materials as the CIT-9 peaks are clearly shifted to the right, to lower ppm values (Figures S17–S20). Also, it is more difficult to prepare the cationic polymer based on 1,4-diazabicyclo[2.2.2]-octane (dabco), and its cost likely excludes commercial-scale implementation. CIT-9, in contrast, is made with a simple organic from precursor molecules common in the amine industry.[7,18] Finally, K-CIT-9 was subjected to steaming treatments (up to 700 °C with 47 kPa of steam partial pressure) where the GME framework proved to be fully stable (see PXRD and ^{29}Si-NMR in Figures S21 and S22) underscoring its hydrothermal stability.

In conclusion, a new GME-zeolite has been discovered,[19] by using a facile and cost-effective route. The synthesis involves a very sensitive reaction system which either produces the channel-based GME or cage-based AEI zeolite when only using a *cis*-isomer. The former is promoted by high concentration of the OSDA, likely inducing its close line-up in the 12MR channel. The dilute conditions lead to OSDA included in an AEI cage. Molecular modelling provides a possible explanation for the synthesis results as the *cis*-isomer showed a seemingly perfect fit in the main channel of the GME zeolite. Compared to all existing GME materials, CIT-9 has less Al, a higher pore volume, and no stacking faults or disorder. These key features are crucial when considering the GME zeolite topology for catalytic applications. At high temperature, the GME framework transforms into AFI unless K^+-exchanged. The mechanisms of this phase-change were elucidated for the first time and occurs at 280–330 °C.

Acknowledgements

M.D. thanks the Research Foundation - Flanders (FWO) and BOFZAP for funding. SACHEM Inc. and PQ Corporation are thanked for providing the piperidinium OSDA and sodium silicate, respectively. Tom Rea and Maryam Deldar are thanked for RED and variable temperature PXRD

respectively. Most of the work performed at Caltech was supported by Chevron Energy Technology Company. Dr. Stacey Zones is thanked for insightful discussions.

Conflict of interest

The authors declare no conflict of interest.

Keywords: AFI zeolite · gmelinite · organic structure-directing agents · rotation electron diffraction · zeolites

How to cite: *Angew. Chem. Int. Ed.* **2017**, *56*, 13475–13478
Angew. Chem. **2017**, *129*, 13660–13663

[1] a) M. E. Davis, *Chem. Mater.* **2014**, *26*, 239–245; b) M. Moliner, C. Martínez, A. Corma, *Angew. Chem. Int. Ed.* **2015**, *54*, 3560–3579; *Angew. Chem.* **2015**, *127*, 3630–3649.
[2] a) W. Vermeiren, J. P. Gilson, *Top. Catal.* **2009**, *52*, 1131–1161; b) A. Corma, *Chem. Rev.* **1995**, *95*, 559–614.
[3] a) L. Bui, H. Luo, W. R. Gunther, Y. Román-Leshkov, *Angew. Chem. Int. Ed.* **2013**, *52*, 8022–8025; *Angew. Chem.* **2013**, *125*, 8180–8183; b) M. Dusselier, P. Van Wouwe, A. Dewaele, P. A. Jacobs, B. F. Sels, *Science* **2015**, *349*, 78–80.
[4] a) U. Olsbye, S. Svelle, M. Bjørgen, P. Beato, T. V. W. Janssens, F. Joensen, S. Bordiga, K. P. Lillerud, *Angew. Chem. Int. Ed.* **2012**, *51*, 5810–5831; *Angew. Chem.* **2012**, *124*, 5910–5933; b) A. M. Beale, F. Gao, I. Lezcano-Gonzalez, C. H. F. Peden, J. Szanyi, *Chem. Soc. Rev.* **2015**, *44*, 7371–7405.
[5] R. H. Daniels, G. T. Kerr, L. D. Rollmann, *J. Am. Chem. Soc.* **1978**, *100*, 3097–3100.
[6] O. Chiyoda, M. E. Davis, *Microporous Mesoporous Mater.* **2000**, *38*, 143.
[7] M. Dusselier, J. E. Schmidt, R. Moulton, B. Haymore, M. Hellums, M. E. Davis, *Chem. Mater.* **2015**, *27*, 2695–2702.
[8] a) M. Dusselier, M. A. Deimund, J. E. Schmidt, M. E. Davis, *ACS Catal.* **2015**, *5*, 6078–6085; b) R. Ransom, J. Coote, R. Moulton, F. Gao, D. F. Shantz, *Ind. Eng. Chem. Res.* **2017**, *56*, 4350–4356.
[9] T. M. Davis, A. T. Liu, C. M. Lew, D. Xie, A. I. Benin, S. Elomari, S. I. Zones, M. W. Deem, *Chem. Mater.* **2016**, *28*, 708–711.
[10] A. Burton, G. Lee, S. I. Zones, *Microporous Mesoporous Mater.* **2006**, *90*, 129.
[11] a) M. Moliner, C. Franch, E. Palomares, M. Grill, A. Corma, *Chem. Commun.* **2012**, *48*, 8264–8266; b) P. Wagner, et al., *J. Am. Chem. Soc.* **2000**, *122*, 263–273; c) S. I. Zones, Y. Nakagawa, S. T. Evans, G. S. Lee, US5958370, **1999**.
[12] Q. Huo, US6423295, **2002**.
[13] A. Alberti, I. Parodi, G. Cruciani, M. C. Dalconi, A. Martucci, *Am. Mineral.* **2010**, *95*, 1773–1782.
[14] a) R. F. Lobo, M. E. Davis, *Microporous Mater.* **1994**, *3*, 61–69; b) R. Bialek, W. M. Meier, M. Davis, M. J. Annen, *Zeolites* **1991**, *11*, 438–442.
[15] a) A. Ito, H. Maekawa, H. Kawagoe, K. Komura, Y. Kubota, Y. Sugi, *Bull. Chem. Soc. Jpn.* **2007**, *80*, 215–223; b) Y. Kubota, H. Maekawa, S. Miyata, T. Tatsumi, Y. Sugi, *Microporous Mesoporous Mater.* **2007**, *101*, 115.
[16] E. Mielczarski, S. B. Hong, R. Davis, M. Davis, *J. Catal.* **1992**, *134*, 359.
[17] Q. Huo, N. A. Stephenson, US6632767, **2003**.
[18] a) M. Dusselier, M. E. Davis, J. E. Schmidt, US Patent 20160122192 A1, **2016**; b) E. F. V. Scriven, R. Murugan, *Kirk-Othmer Encyclopedia of Chemical Technology*, Wiley, New York, **2000**.
[19] M. Dusselier, M. E. Davis, US20160243532, **2016**.

Manuscript received: July 21, 2017
Revised manuscript received: August 25, 2017
Accepted manuscript online: August 30, 2017
Version of record online: September 21, 2017

